International Journal of Engineering Science 146 (2020) 103183

Contents lists available at ScienceDirect

International Journal of Engineering Science

journal homepage: www.elsevier.com/locate/ijengsci

On stress singularity near the tip of a crack with surface stresses

Nikolai Gorbushin[a], Victor A. Eremeyev[b,c,*], Gennady Mishuris[d]

[a] Ecole Superieure de Physique et de Chimie Industrielles de la Ville de Paris, 10 Rue Vauquelin, Paris, Ile-de-France, France
[b] Gdańsk University of Technology, Gdańsk, Poland
[c] R. E. Alekseev Nizhny Novgorod Technical University, Minin St., 24, Nizhny Novgorod 603950, Russia
[d] Aberystwyth University, Ceredigion SY23 3BZ, Wales, UK

ARTICLE INFO

Article history:
Received 10 October 2019
Revised 14 October 2019
Accepted 17 October 2019

Keywords:
Mode III crack
Surface stresses
Nonhomogeneous surface properties
Wiener–Hopf equation

ABSTRACT

In the framework of the simplified linear Gurtin–Murdoch surface elasticity we discuss a singularity of stresses and displacements in the vicinity of a mode III crack. We show that inhomogeneity in surface elastic properties may significantly affect the solution and to change the order of singularity. We also demonstrate that implicitly or explicitly assumed symmetry of the problem may also lead to changes in solutions. Considering various loading and symmetry conditions we show that the stresses may have logarithmic or square root singularity or be bounded in the vicinity of a crack tip.

Introduction

It is well established that the surface related phenomena become important when the ratio of number of near-surface material particles (“atoms”) to one in the bulk becomes significant as in the case of nanostructured materials. Various enhancements of classic elasticity have been proposed in order to capture deviations of material properties at the nanoscale from the microscopic ones. In particular, there is a so-called size-effect, that is the dependence of material properties such as Young’s modulus on the characteristic size. To this end, we mention the surface elasticity model proposed by Gurtin and Murdoch (1975, 1978) that has found various applications in mechanics at the nanoscale, see, e.g., Duan, Wang, and Karihaloo (2008), Wang et al. (2011) and Eremeyev (2016). From the physical point of view, this model describes deformations of an elastic solid with a thin near-surface layer which elastic moduli differ from ones in the bulk material. The layer is modelled as a infinitesimally thin elastic coating attached to the surface. The constitutive equations for the bulk material and for the coating are formulated independently. Mathematically, the governing equations for the coating coincide with ones of a hyperelastic membrane. As a result, in the case of small deformations and an isotropic material we have two additional elastic moduli called the surface elastic Lamé moduli. These moduli inherit both thickness and elastic properties of the near-surface layer. The stress resultants in limiting *membrane* are called surface stresses and are similar to surface tension known in the theory of capillarity. From the mathematical point of view, the presence of surface stresses results in changes of the smoothness of the classic and weak solutions, see Schiavone and Ru (2009), Eremeyev and Lebedev (2013) and

* Corresponding author at: Gdańsk University of Technology, Gdańsk, Poland.
E-mail addresses: nikolai.gorbushin@espci.fr (N. Gorbushin), eremeyev.victor@gmail.com (V.A. Eremeyev), ggm@aber.ac.uk (G. Mishuris).

https://doi.org/10.1016/j.ijengsci.2019.103183

Sigaeva and Schiavone (2014) and references therein. For example, weak solutions of the boundary-value problems for solids with surface stresses belong to Sobolev's spaces containing generalized functions which under sufficiently general conditions are smoother than in the case of linear elasticity (Eremeyev & Lebedev, 2016). Let us note that the case of cracks does not satisfy these conditions and because of this the question of the singularity near the crack tip remains still open.

In literature, the surface elasticity equations have been used to extend classic linear fracture mechanics, in particular, to analysis of stress concentration near crack tips, see, e.g., Antipov and Schiavone (2011), Kim, Schiavone, and Ru (2011c), Kim, Ru, and Schiavone (2013) and Walton (2012), including, also, bridged cracks, see Wang and Schiavone (2016a) and Wang and Wang (2017), and curvilinear cracks Wang (2015). Mode III crack was analyzed in details by Kim, Schiavone, and Ru (2010b), Kim, Schiavone, and Ru (2010a) and Kim, Schiavone, and Ru (2011b) where complex variable methods were used to obtain an exact solution valid everywhere including the vicinity of cracks tips. These results shown that unlike classic linear elasticity the stresses may remain finite at the crack tip that is more realistic from the physical point of view. On the other hand in some cases the surface stresses cannot eliminate the singularity, see Walton (2012), Kim et al. (2013), Wang and Schiavone (2016b) and Li (2019). In most of the above mentioned works the surface elastic moduli were assumed to be constant. Wang and Schiavone (2015, 2016b) demonstrated that inhomogeneity of the surface elastic moduli may also significantly affect the corresponding solutions. Note that mathematically, the corresponding boundary conditions are equivalent to the so-called stiff interface between materials discussed by Benveniste and Miloh (2001) and Benveniste and Miloh (2007), see also Mishuris, Öchsner, and Kuhn (2006a). Singularity near the tip of the interfacial crack dynamically growing along the stiff interface was investigated by Mishuris, Movchan, and Movchan (2006b) and Mishuris, Movchan, and Movchan (2010); the static problem of an interfacial crack lying at a stiff interface of arbitrary shape and elastic properties near the crack tip was analyzed by Mishuris (2003).

The present paper focuses on the issue of stress singularity at a crack tip with the account of surface stresses along the crack surfaces. The analysis is restricted to a relatively simple problem of stress concentrations in the vicinity of mode III crack. The considered inhomogeneity of the surface elastic moduli represents the concentration of surface strain energy near the crack tip. It also covers two limiting cases, of traction-free and of rigidly stiff interface.

The paper is organized as follows. In Section 1 a brief overview of the basic equations of elastostatics in the framework of the linear Gurtin–Murdoch model. In Section 2 the problem of anti-plane deformations of an elastic half-space with a crack is formulated; this problem is split into symmetric and asymmetric (with respect to crack line) problems. The formulation of the symmetric problem in terms of the Mellin is reformulated in terms of the Wiener–Hopf problem in Section 3. The analysis of obtained solution is given in Section 4. We discuss the case when stresses have the logarithmic singularity near the crack tip and when they are bounded. We also discuss two limiting cases, of zero surface stresses and of a rigid inclusion ("anticrack"). Numerical example of stress and displacement distributions is presented in Section 5. The solution of the asymmetric problem is analyzed in Section 6, where we identify the square root stress singularity and calculate the stress intensity factor. We believe that this analysis effectively closes discussions on disparity of results in various papers concerning singularity at the crack tip with surface stress on its surfaces.

1. Basics of linear Gurtin–Murdoch model

Following Gurtin and Murdoch (1975) we introduce the basic equations as follows. In the bulk, we have classic constitutive equations of an isotropic solid with Hooke's law

$$\boldsymbol{\sigma} = 2\mu\mathbf{e} + \lambda\,\mathbf{I}\,\mathrm{tr}\,\mathbf{e}, \quad \mathbf{e} = \frac{1}{2}\left(\nabla\mathbf{u} + (\nabla\mathbf{u})^T\right),$$

where λ and μ are Lamé elastic moduli, $\boldsymbol{\sigma}$ is the stress tensor, $\mathbf{e}$ is the strain tensor, $\mathbf{u} = \mathbf{u}(\mathbf{x})$ is a displacement vector, $\mathbf{x}$ is the position vector, tr is the trace operator, $\mathbf{I}$ is the 3D unit tensor, and ∇ is the 3D nabla-operator.

Additionally, we introduce surface stress tensor $\mathbf{s}$ defined as follows

$$\boldsymbol{\tau} = \mu_s\boldsymbol{\epsilon} + \lambda_s\mathbf{P}(\mathrm{tr}\,\boldsymbol{\epsilon}), \quad \boldsymbol{\epsilon} = \frac{1}{2}\left(\mathbf{P}\cdot(\nabla_s\mathbf{u}) + (\nabla_s\mathbf{u})^T\cdot\mathbf{P}\right),$$

where λ_s and μ_s are the surface elastic moduli, $\nabla_s = \mathbf{P}\cdot\nabla$ is the surface nabla operator, $\mathbf{P} \equiv \mathbf{I} - \mathbf{n}\otimes\mathbf{n}$, $\mathbf{n}$ is the unit vector of outer normal to ∂V, where ∂V is the boundary of the body volume V.

Considering mass force free solid we get the equilibrium equation

$$\nabla\cdot\boldsymbol{\sigma} = \mathbf{0}, \quad \forall\,\mathbf{x}\in V, \tag{1}$$

and the static boundary equations

$$\mathbf{n}\cdot\boldsymbol{\sigma} = \nabla_s\cdot\boldsymbol{\tau} + \mathbf{g}, \quad \forall\,\mathbf{x}\in\partial V, \tag{2}$$

where $\mathbf{g}$ is a traction vector. The latter equation differs from the classic traction condition in linear elasticity. It called the generalized Laplace–Young equation. As a result, the term with $\boldsymbol{\tau}$ brings new properties of corresponding solutions of the boundary-value problem (1) and (2).

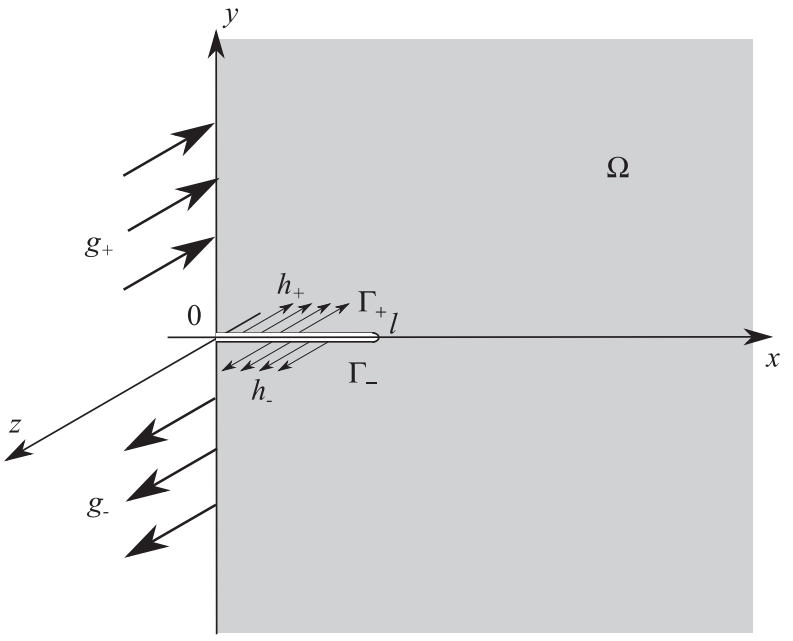

Fig. 1. An elastic half-space $x > 0$ with a crack of length l.

2. Anti-plane problem formulation

We consider mode III plane fracture problem in a half-space $x > 0$ within the Oxy frame. A crack of length l occupies an interval $0 < x < l$, $y = 0$ and loaded by a specific type of shear traction, see Fig. 1. On the boundary of the half plane ($y = 0$) and the crack surfaces ($\Gamma_\pm$), the shear stresses are imposed.

For the anti-plane deformations, the vectors of displacements and external forces takes the form

$$\mathbf{u} = w(x,y)\mathbf{i}_3, \quad \mathbf{g} = \begin{cases} -g_+(y)\mathbf{i}_3; & x = 0, \quad y > 0; \\ g_-(y)\mathbf{i}_3; & x = 0, \quad y < 0; \\ -h_+(x)\mathbf{i}_3; & x \in (0,l), \quad y = 0+; \\ h_-(x)\mathbf{i}_3; & x \in (0,l), \quad y = 0-, \end{cases} \tag{3}$$

where $\mathbf{i}_k$, $k = 1, 2, 3$ are base unit vectors related to Cartesian coordinates x, y, z, respectively.

For the anti-plane shear deformation (3), the equilibrium Eq. (1) and boundary conditions (2) reduce to the Laplace equation into the domain Ω

$$\nabla^2 w = 0, \qquad x, y \in \Omega, \tag{4}$$

and the boundary conditions

$$\sigma_{xz} = g_\pm(y), \quad x = 0, \ \pm y > 0, \tag{5}$$

$$\sigma_{yz} + \frac{\partial}{\partial x}\left(f(x)\frac{\partial w}{\partial x}\right) = h_\pm(x), \quad 0 < x < l, \quad y = \pm 0, \tag{6}$$

$$[w] = 0, \quad [\sigma_{\theta z}] = 0, \quad x > l, \quad y = \pm 0, \tag{7}$$

respectively.

Note that more general linear constitutive equations for $\boldsymbol{\tau}$ can be also considered (Duan et al., 2008), see also Ru (2010). For example, they include residual surface stress $\sigma_0\mathbf{P}$. However, the appearance of σ_0 does not change the form of (6), see, e.g., Kim et al. (2010b).

In these equations $w = w(x,y)$ is a displacement field in z direction, $\sigma_{yz} = \mu\partial w/\partial y$, $\sigma_{xz} = \mu\partial w/\partial x$ are shear stresses. Functions $g_\pm(y), h_\pm(x)$ define the loading conditions and the function $\mu_s \equiv f(x)$ describes the nonhomogeneous surface shear modulus. The case $f(x) = C \equiv \text{const}$ is the standard case of the homogeneous surface elastic properties, see e.g., Kim et al. (2010a,b, 2011b), whereas $f(x) = Cx$ corresponds to the assumption that the surface stresses are most important in the neighbourhood of the crack tip. In certain sense this assumption is similar to Barenblatt's model of cracks with adhesion zone (Barenblatt, 1959). We consider here only this case to highlight possible consequence of such realistic assumption, when the surface energy is mostly concentrated near the crack tip and vanishes far from it.

We assume that the given functions do not affect directly the behaviour in crack singular points. Namely, we state that $g_{\pm}(x)$ are finite functions ($g_{\pm}(x)=0$ for $|x|<\varepsilon$, and $|x|>1/\varepsilon$ for some $\varepsilon>0$), while the functions $h_{\pm}(x)$, described on the crack surface, are finite and smooth enough ($h_{\pm}\in C_0^1[0,l]$).

We search for a solution where the displacement and stresses both vanish at infinity in the same manner as for the problem for half-space without a crack:

$$w=O(r^{-1}),\quad \sigma_{jz}=O(r^{-2}),\quad r\to\infty. \tag{8}$$

Using the superposition principle, we divide the problem into two: symmetrical and antisymmetrical with respect to the ray $\theta=0$ ($y=0$, $x>0$ and the respective problem can be considered in the domain $0<\theta<\pi/2$ with the respectively modified function $g_+(y)=g_j(y)$ ($j=1,2$ $2g_1(y)=g_+(y)+g_-(-y)$ and $2g_2(y)=g_+(y)-g_-(-y)$, $y>0$, while the boundary conditions defined along the ray $\theta=0$ read:

$$\sigma_{yz}+C\frac{\partial}{\partial x}\left(x\frac{\partial w}{\partial x}\right)=h_1(x),\quad 0<x<l,\quad w=0,\quad x>l,\quad y=0. \tag{9}$$

and

$$\sigma_{yz}+C\frac{\partial}{\partial x}\left(x\frac{\partial w}{\partial x}\right)=h_2(x),\quad 0<x<l,\quad w'_{\theta}=0,\quad x>l,\quad y=0, \tag{10}$$

where $2h_1(x)=h_+(x)+h_-(x)$ and $2h_2(x)=h_+(x)-h_-(x)$.

The mathematical treatment of the problem becomes easier if we turn to the polar coordinates. The Eq. $(5)_1$ reads:

$$\left(\frac{1}{r^2}\frac{\partial}{\partial\theta^2}+\frac{1}{r}\frac{\partial}{\partial r}\left(r\frac{\partial}{\partial r}\right)\right)w=0,\qquad r>0,\quad 0<\theta<\frac{\pi}{2}, \tag{11}$$

with the boundary conditions

$$\sigma_{\theta z}\big|_{\theta=\pi/2}=\frac{\mu}{r}\frac{\partial w}{\partial\theta}\Big|_{\theta=\pi/2}=g_j(r),\quad r>0,\quad j=1,2, \tag{12}$$

along the boundary $\theta=\pm\frac{\pi}{2}$ and

$$\begin{aligned}
&\sigma_{\theta z}+C\frac{\partial}{\partial r}\left(r\frac{\partial w}{\partial r}\right)=h_1(r),\quad 0<r<l,\quad w=0,\quad r>l,\quad \theta=0,\\
&\sigma_{\theta z}+C\frac{\partial}{\partial r}\left(r\frac{\partial w}{\partial r}\right)=h_2(r),\quad 0<r<l,\quad \sigma_{\theta z}=0,\quad r>l,\quad \theta=0,
\end{aligned} \tag{13}$$

along the other boundary. Here indices 1 and 2 correspond to the symmetric and asymmetric problem, respectively. In what follows we omit these indices referring explicitly to the problem under consideration. Note that the estimate 8 can be different in those two cases and defines the worst behaviour.

It is convenient to perform normalization as follows:

$$\hat r=\frac{r}{l},\quad \hat g(\hat r)=g(\hat r l)l,\quad \hat h(\hat r)=h(\hat r l)l,\quad \hat w(\hat r,\theta)=w(\hat r l,\theta). \tag{14}$$

We drop hats in the following, if not mentioned the opposite. Note that the crack length $l>0$ is not appeared in the problem formulation as all the operator are homogeneous of the same order. However, that value of course is a part of the solution influencing the new right-hand sides.

3. Solution for the symmetric problem

3.1. Reduction to the Wiener–Hopf problem

Let us write the boundary conditions in the form defined along the entire ray $0<r<\infty$:

$$\begin{aligned}
&\mu\frac{\partial w}{\partial\theta}=rg(r),\quad \theta=\frac{\pi}{2},\\
&\mu\frac{\partial w}{\partial\theta}+Cr\frac{\partial}{\partial r}\left(r\frac{\partial w}{\partial r}\right)=rh(r)+\phi(r),\quad w=\psi(r),\quad \theta=0.
\end{aligned} \tag{15}$$

where the given function $h(r)$ satisfies the condition $h(r)=0$ for $r>1$ and newly introduced unknown functions are assumed to be:

$$\phi(r)=0,\quad 0<r<1,\qquad \psi(r)=0,\quad r>1. \tag{16}$$

Note that for simplicity we omit here index in the functions h_1 and g_1. An additional condition for those functions near the end of the intervals, where they do not vanish, will be prescribed later.

In this particular case one may apply the Mellin transform in the standard form and its application to the displacement is defined as:

$$W(s,\theta)=\int_0^\infty w(r,\theta)r^{s-1}\,dr,$$

Application of this transform to (15) leads to:

$$\begin{array}{l}\frac{\partial^2 W}{\partial\theta^2}(s,\theta)+s^2W(s,\theta)=0,\quad 0<\theta<\frac{\pi}{2}\\ \quad\mu\frac{\partial W}{\partial\theta}(s,\theta)=G(s+1),\quad \theta=\frac{\pi}{2}\end{array}\tag{17}$$

$$\mu\frac{\partial W}{\partial\theta}(s,\theta)+Cs^2W(s,\theta)=H^+(s+1)+\Phi^-(s),\quad W(s,\theta)=\Psi^+(s),\quad \theta=0.\tag{18}$$

Here, the known functions are:

$$G(s+1)=\int_0^\infty g(r)r^s\,dr,\quad H^+(s+1)=\int_0^1 h(r)r^s\,dr,\tag{19}$$

and unknown functions are defined as follows:

$$\Psi^+(s)=\int_0^1\psi(r)r^{s-1}\,dr,\quad \Phi^-(s)=\int_1^\infty\phi(r)r^{s-1}\,dr.\tag{20}$$

We search for solution $w(r)$ satisfying the following conditions at all singular points of the problem:

$$w(r)=w_0+O(r^{\alpha_0}),\quad r\to 0,\tag{21}$$
$$w(r)=O((1-r)^{\alpha_1}),\quad r\to 1-,\tag{22}$$
$$w(r)=O(r^{-\alpha_\infty}),\quad r\to\infty,\tag{23}$$

where all unknown constants are positive ($\alpha_0,\ \alpha_1,\ \alpha_\infty>0$). As a result, we expect that:

$$\psi(r)=w_0+O(r^{\alpha_0}),\quad r\to 0,\tag{24}$$
$$\psi(r)=O((r-1)^{\alpha_1}),\quad r\to 1-,\tag{25}$$
$$\phi(r)=O(r^{-\alpha_\infty-1}),\quad r\to\infty,\tag{26}$$
$$\phi(r)=O((1-r)^{\alpha_1-2}),\quad r\to 1+.\tag{27}$$

In turn, we conclude that $\Psi^+(s)$ and $\Phi^-(s)$ are analytic in the half-planes $\Re s>-\alpha_0$ (with a possible simple pole at the point $s=0$) and $\Re s<\alpha_\infty$, respectively. Hereinafter $\Re$ and $\Im$ denote the real and imaginary parts of a complex number, respectively. Moreover, their behaviours at infinity within the respective half-planes can be estimated by the Abelian type theorem (Piccolroaz & Mishuris, 2013; Piccolroaz, Mishuris, & Movchan, 2009) as

$$\Phi^+(s)=O\left(s^{-1-\alpha_1}\right),\quad \Psi^-(s)=O\left(s^{-\alpha_1+1}\right),\quad s\to\infty.\tag{28}$$

For the mechanical equilibrium of the system, the following balance condition should be satisfied:

$$\oint_\Gamma\sigma_{\theta z}d\Gamma=0\quad\text{or}\quad\int_0^\infty g(r)dr-\int_0^\infty\mu\frac{1}{r}\frac{\partial w}{\partial\theta}\Big|_{\theta=0}=0,$$

The latter can be written in terms of the Mellin transform as

$$G(1)=\mu\frac{\partial W}{\partial\theta}(0,0).\tag{29}$$

Solution of the derived differential Eq. $(17)_1$ reads:

$$W(s,\theta)=A(s)\cos\left(s\left(\theta-\frac{\pi}{2}\right)\right)+B(s)\sin\left(s\left(\theta-\frac{\pi}{2}\right)\right),\tag{30}$$

$$\mathcal{M}[\sigma_{z\theta}](s+1,\theta)=\mu\frac{\partial W}{\partial\theta}(s,\theta)=-\mu sA(s)\sin\left(s\left(\theta-\frac{\pi}{2}\right)\right)+s\mu B(s)\cos\left(s\left(\theta-\frac{\pi}{2}\right)\right),\tag{31}$$

with functions $A(s)$ and $B(s)$ analytical in the strip ($0<\Re s<\alpha_\infty$) to be found. We apply boundary condition at $\theta=\pi/2$ and obtain:

$$B(s)=\frac{G(s+1)}{\mu s}.\tag{32}$$

Note that the balance condition (29) transforms into (32) in the limiting case $s\to 0$. Here we take into account the fact that the displacement is bounded at zero point and, therefore, the function $A(s)$ has a simple pole at zero point only. If $G(1)\neq 0$, then $B(s)$ has a simple pole at point $s=0$, however, the image of the displacement is always bounded at this point.

Substituting (30) into the boundary conditions along the ray $\theta = 0$ we get:

$$\begin{pmatrix} A(s) \\ B(s) \end{pmatrix} = \begin{pmatrix} \cos\frac{\pi s}{2} & \sin\frac{\pi s}{2} \\ -\sin\frac{\pi s}{2} & \cos\frac{\pi s}{2} \end{pmatrix} \begin{pmatrix} \Psi^+(s) \\ \dfrac{\Phi^-(s) + H^+(s+1)}{\mu s} - \dfrac{Cs}{\mu}\Psi^+(s) \end{pmatrix} \tag{33}$$

This brings us to the Wiener–Hopf equation:

$$\frac{G(s+1)}{Cs^2\cos\frac{\pi s}{2}} = \frac{1}{s^2 C}\big(\Phi^-(s) + H^+(s+1)\big) - L(s)\Psi^+(s), \tag{34}$$

valid in the strip $-\alpha_0 < \Re s < \alpha_\infty$. Here the kernel function is defined as follows:

$$L(s) = \frac{\mu}{sC}\tan\frac{\pi s}{2} + 1, \tag{35}$$

and takes real positive values bounded from below along the imaginary axis $L(i\xi) \geq L(0) = \mu\pi/(2C) + 1$. Moreover, its behaviour at infinity is estimated as:

$$L(it) = 1 + \frac{\mu}{|t|C} + O\big(|t|^{-1}e^{-\pi|t|/2}\big), \quad t \to \pm\infty. \tag{36}$$

Note that the first zero of the kernel function $L(s)$ in the half-plane $\Re s < 0$ is real ($s = -\beta_*$) where $1 < \beta_*(C) < 2$ such that:

$$L(s) \neq 0, \quad -\beta_* < \Re s < \beta_*,$$

and $\beta_*(C)$ is a monotonically decreasing function with respect to constant $C > 0$ and:

$$\lim_{C\to 0}\beta_*(C) = 2, \quad \lim_{C\to\infty}\beta_*(C) = 1. \tag{37}$$

Note that our assumptions (21)–(23) and (24)–(27) are consistent with (34) and the following conclusions can be made from its analysis at point $s = 0$:

$$G(1) = \Phi^-(0) + H^+(1), \quad w_0 = \frac{1}{CL(0)}\frac{d}{ds}\big(\Phi^-(s) + H^+(s+1) - G(s+1)\big)\big|_{s=0}. \tag{38}$$

The first equation in the latter is nothing else but an alternative form of the balance condition (29).

Further conclusions can be made on the width of the analyticity strip analyzing the Wiener–Hopf equation, providing all given functions are finite:

$$\alpha_\infty = 1, \quad \alpha_0 = \beta_*(C) > 1. \tag{39}$$

3.2. Factorization of the function L(s)

The solution of the Wiener–Hopf problem is closely related with the factorization of the kernel function. Note that $L(s)$ is an even analytical function in the strip $-1 < \Re s < 1$. It has simple poles at $s = \pm 1$ at the borders of this strip and $L(\pm i\infty) = 1$ within the strip. It can be therefore easily factorized in the form:

$$L(s) = L^+(s)L^-(s), \quad L^-(s) = L^+(-s), \quad L^+(0) = \sqrt{\frac{\mu\pi}{2C} + 1}, \quad \lim_{s\to\pm i\infty} L^\pm(s) = 1, \tag{40}$$

and

$$L^\pm(s) = \exp\left\{\mp\frac{1}{2\pi i}\int_{-i\infty\mp\gamma}^{i\infty\mp\gamma}\frac{\log(L(\xi))}{\xi - s}d\xi\right\}, \tag{41}$$

where $0 \leq \gamma < 1$ is an arbitrary constant. The function $L^+(s)$ is analytic in the complex half-plane $-1 < \Re s < \infty$. Unfortunately, factorization can not be accomplished in the closed form and numerical evaluation of the factors is required. We can estimate more accurately the behaviour of the factors $L^\pm(s)$ at infinity. Let us consider an auxiliary function

$$\chi(t, b) = \frac{a}{|t| + b}, \quad a = \frac{\mu}{C}, \tag{42}$$

while $b > 0$ should be found from the condition

$$T(b) \equiv \int_0^\infty \Big(\log L(it) - \chi(t, b)\Big)dt = 0. \tag{43}$$

One can check that

$$\log L(it) - \chi(t) = O\big(|t|^{-2}\big), \quad t \to \infty,$$

thus the integral in (43) is finite for any $0 < b < \infty$, while the function $T(b)$ monotonically increase from $-\infty$ to ∞ when b changes from 0 to ∞. Therefore, there exists a unique $b = b_0 > 0$ giving $T(b_0) = 0$.

As a result, we can represent the factors $L^{\pm}(s)$ in the form:

$$L^{\pm}(s) = L_0^{\pm}(s)L_*^{\pm}(s), \quad L_*^{\pm}(s) = \exp\left\{\mp\frac{1}{2\pi}\int_{-\infty}^{\infty}\frac{\log L(it) - \chi(t,b_0)}{it-s}dt\right\}, \tag{44}$$

and

$$L_0^{\pm}(s) = \exp\left\{\mp\frac{1}{2\pi}\int_{-\infty}^{\infty}\frac{\chi(t,b_0)}{it-s}dt\right\} = \exp\left\{\pm\frac{s}{\pi}\int_0^{\infty}\frac{\chi(t,b_0)}{t^2+s^2}dt\right\},$$

or

$$L_0^{\pm}(s) = \exp\left\{\frac{a}{2\pi}\frac{\pi b_0 \pm 2s\log(\pm s/b_0)}{s^2+b_0^2}\right\}, \tag{45}$$

Note that $\log z$ here is the same function with the cut along the negative part of the real axis.

The behaviour of $L_*^{\pm}(s)$ is now estimated (in the respective half-plane) as:

$$L_*^{\pm}(s) = 1 + o\big(s^{-1}\big), \quad L_0^{\pm}(s) = 1 \pm \frac{a}{\pi s}\big(\log(\pm s) - \log b_0\big) + o\big(s^{-1}\big), \quad s\to\infty. \tag{46}$$

Summarizing these intermediate results we conclude that the leading terms of the asymptotic behaviour of the functions $L^{\pm}(s)$ and $L_0^{\pm}(s)$ coincides and:

$$L^{\pm}(s) = 1 \pm \frac{\mu}{\pi sC}\big(\log(\pm s) - \log b_0\big) + o\big(s^{-1}\big), \quad s\to\infty. \tag{47}$$

Remark: note that the term of the order s^{-1} can be computed differently. Indeed, it is enough to take any value $b>0$ then the asymptotics (47) takes form:

$$L^{\pm}(s) = 1 \pm \frac{\mu}{\pi sC}\left(\log(\pm s) - \log b + \frac{C}{\mu}T(b)\right) + o\big(s^{-1}\big), \quad s\to\infty,$$

or $b_0 = b\exp(-CT(b)/\mu)$.

3.3. Solution of the problem

Having in place the factorization of the kernel, the Wiener–Hopf Eq. (34) can be rewritten in the equivalent form:

$$\frac{1}{CL^-(s)}\Phi^-(s) - s^2L^+(s)\Psi^+(s) = \frac{F(s)}{C}, \tag{48}$$

in the strip $0<\Re s<1$, where

$$F(s) = \frac{1}{L^-(s)}\left(\frac{1}{\cos\frac{\pi s}{2}}G(s+1) - H^+(s+1)\right). \tag{49}$$

Under the assumptions on the given loads, $F(s)$ is an analytical function at least in the strip $-1<\Re s<1$ and decays at infinity faster than s^{-1}. By means of the standard procedure involving Cauchy type integrals, it can be represented in the form:

$$F(s) = F^+(s) + F^-(s), \quad F^{\pm}(s) = \mp\frac{1}{2\pi i}\int_{-i\infty\mp\gamma}^{i\infty\mp\gamma}\frac{F(\xi)}{\xi - s}d\xi, \tag{50}$$

where $0\le\gamma<1$. Moreover, $F^{\pm}(s)\sim\pm F_{\infty}s^{-1}$ as $|s|\to\infty$ in the respective half-plane.

$$F_{\infty} = \frac{1}{2\pi}\int_{\infty}^{\infty}F(i\xi)d\xi.$$

With this representation in mind, the Wiener–Hopf Eq. (48) can be rewritten in the equivalent form:

$$\frac{1}{L^-(s)}\Phi^-(s) - F^-(s) = s^2CL^+(s)\Psi^+(s) + F^+(s) \equiv \mathcal{P}_n(s), \tag{51}$$

in the strip $0<\Re s<1$, where $\mathcal{P}_n(s)$ is a polynomial according to Liouville's theorem. As a result, the final solution of the Wiener–Hopf equation is:

$$\Psi^+(s) = \frac{\mathcal{P}_n(s) - F^+(s)}{Cs^2L^+(s)}, \quad \Phi^-(s) = \big(F^-(s) + \mathcal{P}_n(s)\big)L^-(s). \tag{52}$$

Comparing this with (28), one can conclude that the degree of the polynomial $n=0$ which delivers two possible scenarios. Note that the case $n=1$ is equivalent to $\alpha_1=0$ and thus, there appears a jump of the displacement near the crack tip that makes no physical sense.

At this point we can find the function $A(s)$ which together with that $B(s)$ defined in (32) and (33) allows us to reconstruct the entire solution:

$$A(s) = -\frac{G(s+1)}{Cs^2L(s)}\left(1 - \frac{Cs}{\mu}\tan\frac{\pi s}{2}\right) + \frac{\Phi^-(s) + H^+(s+1)}{Cs^2L(s)\cos\frac{\pi s}{2}}, \tag{53}$$

Substituting the results into relations for the displacement and stresses in their Mellin leads to:

$$W(s,\theta) = \frac{1}{Cs^2L(s)\cos\frac{\pi s}{2}}\left(\left(\Phi^-(s) + H^+(s+1)\right)\cos s\left(\theta - \frac{\pi}{2}\right) + G(s+1)\left(\frac{Cs}{\mu}\sin s\theta - \cos s\theta\right)\right)$$

$$\mu\frac{\partial}{\partial\theta}W(s,\theta) = \frac{-\mu}{CsL(s)\cos\frac{\pi s}{2}}\left(\left(\Phi^-(s) + H^+(s+1)\right)\sin s\left(\theta - \frac{\pi}{2}\right) - G(s+1)\left(\frac{Cs}{\mu}\cos s\theta + \sin s\theta\right)\right)$$

From the Mellin transform of the boundary conditions in (18) it straightforward follows that for $\theta = 0$:

$$W(s,0) = \Psi^+(s,0),$$

$$\mu\frac{\partial W}{\partial\theta}(s,0) = H^+(s+1) + \Phi^-(s) - Cs^2\Psi^+(s),$$

where functions $\Phi^-(s)$ and $\Psi^+(s)$ are found in (52). It is convenient to present the solution as:

$$W(s,0) = \frac{\mathcal{P}_n(s) - F^+(s)}{Cs^2L^+(s)}, \tag{54}$$

$$\mu\frac{\partial W}{\partial\theta}(s,0) = \Sigma^+(s) + \Sigma^-(s), \tag{55}$$

where

$$\Sigma^+(s) = \frac{F^+(s)}{L^+(s)} + \mathcal{P}_n(s)\left(1 - \frac{1}{L^+(s)}\right) + H^+(s+1) + \mathcal{Q}_{n-1}(s),$$
$$\Sigma^-(s) = F^-(s)L^-(s) + \mathcal{P}_n(s)\left(L^-(s) - 1\right) - \mathcal{Q}_{n-1}(s), \tag{56}$$

with an arbitrary polynomial $\mathcal{Q}_{n-1}(s)$. Finally, note the balance of the external load (38) can be written in the form:

$$G(1) = \Sigma^+(0) + \Sigma^-(0). \tag{57}$$

4. Analysis of the symmetric problem

4.1. Behaviour at infinity

One can directly check that the balance condition (29) is valid when

$$\mathcal{P}_n(0) = F^+(0). \tag{58}$$

Interestingly, the same condition eliminates logarithmic singularity near the point $r = 0$. One can also check that the condition (58) makes both equations in (38) satisfied.

Analyzing the behaviour of the function $\Sigma^-(s)$ we observe that, under the assumptions made on the externally applied load, they are analytic in the domains $\Re s < 1$. This means that our previous statement (39) is valid indeed, $\alpha_\infty = 1$, regardless of the other problem parameters. Thus

$$\sigma_{\theta z}(r,\theta) = O(r^{-2}), \quad r \to \infty.$$

Note that the degree of the polynomial $\mathcal{P}_n(s)$ is restricted by the behaviour of the displacement image at infinity, that gives $n \le 1$, and taking into account the condition (58) we conclude $\mathcal{P}_n(s) = D_0 + D_1 s$ where the constant D_0 as been already defined ($D_0 = F^+(0)$), while the remaining one, D_1, is still to be determined.

Let us consider the case when $D_1 = 0$ for which $\mathcal{Q}_{n-1}(s) = 0$. We get

$$W(s,0) = \frac{F^+(0) - F^+(s)}{Cs^2L^+(s)}, \quad \mu\frac{\partial W}{\partial\theta}(s,0) = \Sigma^+(s) + \Sigma^-(s),$$
$$\Sigma^+(s) = \frac{F^+(s)}{L^+(s)} + F^+(0)\left(1 - \frac{1}{L^+(s)}\right) + H^+(s+1),$$
$$\Sigma^-(s) = F^-(s)L^-(s) + F^+(0)\left(L^-(s) - 1\right). \tag{59}$$

The asymptotic behaviour of these functions is:

$$W(s,0) = \frac{F^+(0)}{Cs^2} + O(s^{-3}\log s), \quad s \to \infty, \tag{60}$$

$$\Sigma^{\pm}(\pm s) = \frac{\mu F^{+}(0)}{\pi C}\frac{\log s}{s} + \frac{1}{s}\left(F_{\infty} - \frac{\mu F^{+}(0)}{\pi C}\log b_0\right) + o(s^{-1}), \quad \Re s \to \pm\infty. \tag{61}$$

As a result, we conclude that

$$w(r,0) = \frac{F^{+}(0)}{C}(1-r) + O\big((1-r)^2\log(1-r)\big), \quad r \to 1-, \tag{62}$$

$$\sigma_{\theta z}(r,0) = -\frac{\mu F^{+}(0)}{\pi C}\log|1-r| + F_{\infty} - \frac{\mu F^{+}(0)}{\pi C}(\log b_0 + \gamma) + o(1), \quad r \to 1. \tag{63}$$

where $\gamma \approx 0.5772$ is the Euler–Mascheroni constant. Finally, near the inlet of the crack we have (compare to (39)):

$$w(r,0) = w_0 + O(r^{\beta_*(C)}), \quad \sigma_{\theta z}(r,0) = O(r^{\beta_*(C)-1}) \quad r \to 0, \tag{64}$$

where

$$w_0 = \sqrt{\frac{2}{C}}\frac{f_0}{\sqrt{\mu\pi + 2C}}, \quad f_0 = -\lim_{s\to 0}\frac{d}{ds}F^{+}(s).$$

If the external load is prescribed in a way that $F^{+}(0) = 0$, then the logarithmic singularity at the crack tip disappears and the smoothness of the displacement further improves. However, the load should be adjusted for each particular value of the constant C. The results correlate nicely with those from (Kim et al., 2013; Wang & Schiavone, 2016b).

4.2. Solution with bounded stress near the crack tip

One can eliminate the stress singularity at the crack tip by considering a solution with $\mathcal{P}_n(s) \equiv 0$. In this case solution becomes:

$$W(s,0) = -\frac{F^{+}(s)}{Cs^2L^{+}(s)}, \quad \mu\frac{\partial W}{\partial\theta}(s,0) = \Sigma^{+}(s) + \Sigma^{-}(s),$$
$$\Sigma^{+}(s) = \frac{F^{+}(s)}{L^{+}(s)} + H^{+}(s+1), \qquad \Sigma^{-}(s) = F^{-}(s)L^{-}(s). \tag{65}$$

And the asymptotic behaviour is:

$$W(s,0) = -\frac{F_{\infty}}{Cs^3} + o(s^{-4}\log s), \quad s \to \infty, \tag{66}$$

$$\Sigma^{+}(s) = \Sigma^{-}(-s) = \frac{1}{s}F_{\infty} + o(s^{-1}), \quad \Re s \to +\infty. \tag{67}$$

In this case

$$w(r,0) = O\big((1-r)^2\log(1-r)\big), \quad r \to 1-, \quad \sigma_{\theta z}(r,0) = F_{\infty} + o(1), \quad r \to 1. \tag{68}$$

However, the function $A(s)$ has then a double pole at zero point. As a result, the displacement has a logarithmic singularity at point $r = 0$, while the stress behaves in the same way as previously:

$$w(r,0) = \frac{-F^{+}(0)}{CL^{+}(0)}\log r + w_0^{*} + O(r^{\beta_*(C)}), \quad \sigma_{\theta z}(r,0) = O(r^{\beta_*(C)-1}) \quad r \to 0, \tag{69}$$

Explanation to this phenomenon is as follows. This solution corresponds to the one with an additional concentrated force applied at zero point from the side of the surface stress ($\theta = 0$, $r = 0$). As a result, the balance condition (29) will now read (compare $(38)_1$):

$$G(1) = H^{+}(1) + \Phi^{-}(0) + \frac{F^{+}(0)}{L^{+}(0)} = \Sigma^{+}(0) + \Sigma^{-}(0) + \frac{F^{+}(0)}{L^{+}(0)}. \tag{70}$$

Note that the last term corresponds to the point force acting at point $r = 0$.

Remark. Note that both solutions discussed in the Sections 4.1 and 4.2 coincide if $F^{+}(0) = 0$.

4.3. Extreme cases $C \to \infty$ and $C \to 0$

Here we only discuss expected behaviour of the solution not concentrating on its exact estimate.

4.3.1. Limit case $C \to \infty$

For the kernel of the Wiener–Hopf equation one can expect:

$$L(s) = 1 + O(C^{-1}), \quad L^{\pm}(s) = 1 + O(C^{-1/2}), \quad C \to \infty, \tag{71}$$

while (compare (37)) in this case $\beta_*(\infty) = 1+$ (and thus the limit is not uniform with respect to variable s). Note that the function $F(s)$ from (48) as well as $F^{\pm}(s)$ can be roughly estimated as

$$F(s) = \frac{G(s+1)}{\cos\frac{\pi s}{2}} + O(C^{-1}), \quad F^{\pm}(s) = O(1), \quad C \to \infty. \tag{72}$$

This gives us

$$\Psi^{+}(s) = O(C^{-1}), \qquad \Phi^{-}(s) = F^{-}(s) = \frac{1}{2\pi i}\int_{-i\infty+\gamma}^{i\infty+\gamma} \frac{G(\xi+1)}{\cos\frac{\pi\xi}{2}}\frac{d\xi}{\xi - s} + o(1), \quad C \to \infty. \tag{73}$$

The first direct conclusion from the latter is that $w(r,0) = O(C^{-1})$ along the entire ray $\theta = 0$ (compare (60)). Along the same line, the stress near the point $r = 0$ will change its behaviour from vanishing to a constant value (see (64)).

Thus, one can expect the solution to *converge* to a solution of the similar problem for a half plane containing no crack. However, *the convergence* should be properly determined.

4.3.2. Limit case $C \to 0$

This case is more difficult to estimate in comparison with the first one.

For the kernel of the Wiener–Hopf equation one can expect:

$$L(s) = O(C^{-1}), \quad L^{\pm}(s) = O(C^{-1/2}), \quad C \to 0, \tag{74}$$

but the estimate is not uniform (remind that $L(s) \to 1$ as $s \to \infty$). Note that the function $F(s)$ from (48) as well as $F^{\pm}(s)$ can be roughly estimated as

$$F(s), F^{\pm}(s) = O(C^{1/2}), \quad C \to 0. \tag{75}$$

This gives us

$$W(s,0) = O(1), \quad \Sigma^{\pm}(s) = (1), \quad C \to 0. \tag{76}$$

Finally, it is clear that the estimate for the solution is blowing up near the point $r = 1$ (compare (62) and (63)). The complete solution is shown in Appendix A for comparative purposes.

5. Numerical example for symmetric problem

We consider the following external load:

$$g(r) = P\delta(r - a), \quad h(r) = 0. \tag{77}$$

As a result, we can conclude that the solution is represented by the formulae (59) with

$$F(s) = \frac{Pa^s}{L^{-}(s)\cos\frac{\pi s}{2}}.$$

It is worth noting that under such loading conditions there exists an exact solution when $C \to \infty$. Indeed, in this case $L(s) = 1$ and one can check that $\Psi^{+}(s) = 0$ while the solution along the boundary reduces to:

$$W(s,0) = 0, \quad \mu\frac{\partial W}{\partial\theta}(s,0) = F(s).$$

We also notice that:

$$\mathcal{M}^{-1}[F(s)](r) = \mathcal{M}^{-1}\left[\frac{G(s+1)}{\cos\frac{\pi s}{2}}\right](r) = \frac{2}{\pi}\frac{Par}{r^2 + a^2}.$$

Thus, we get:

$$w(r,0) = 0, \quad \sigma_{\theta z}(r,0) = \frac{2}{\pi}\frac{Pa}{r^2 + a^2}. \tag{78}$$

In Fig. 2 we present distribution of the stress and displacement along the symmetry line for $\mu = 1$, $P = 1$, $a = 1$ for different properties of the surface stress (various values of $C > 0$). Black solid line corresponds to the limiting case $C = \infty$.

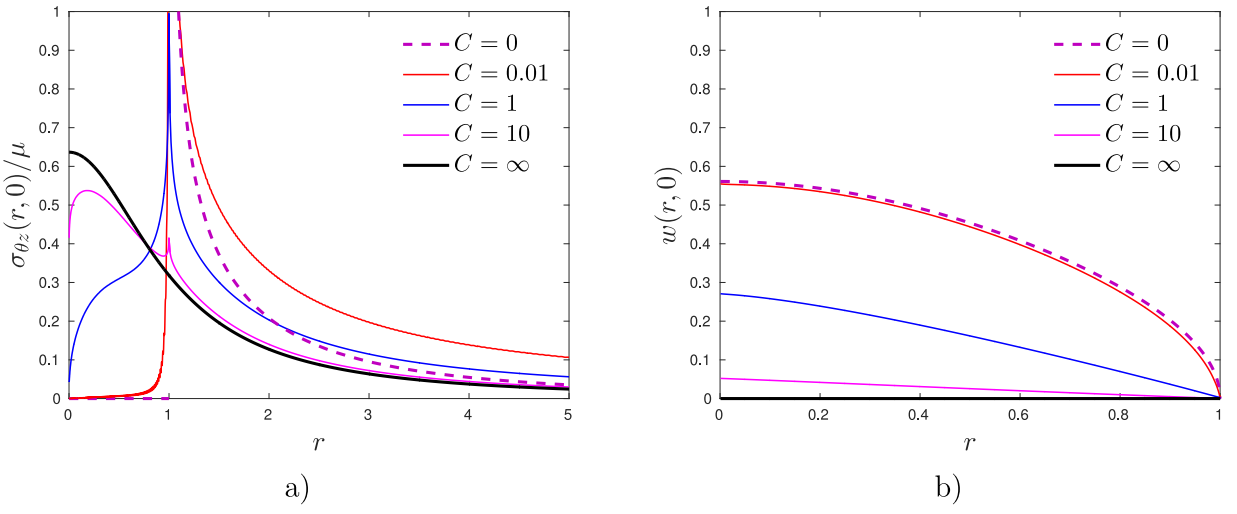

Fig. 2. Logarithmic singularity (Section 4.1). Distribution of stress and displacements according to solution in (64) and different values of C: a) normalized stress, b) displacements.

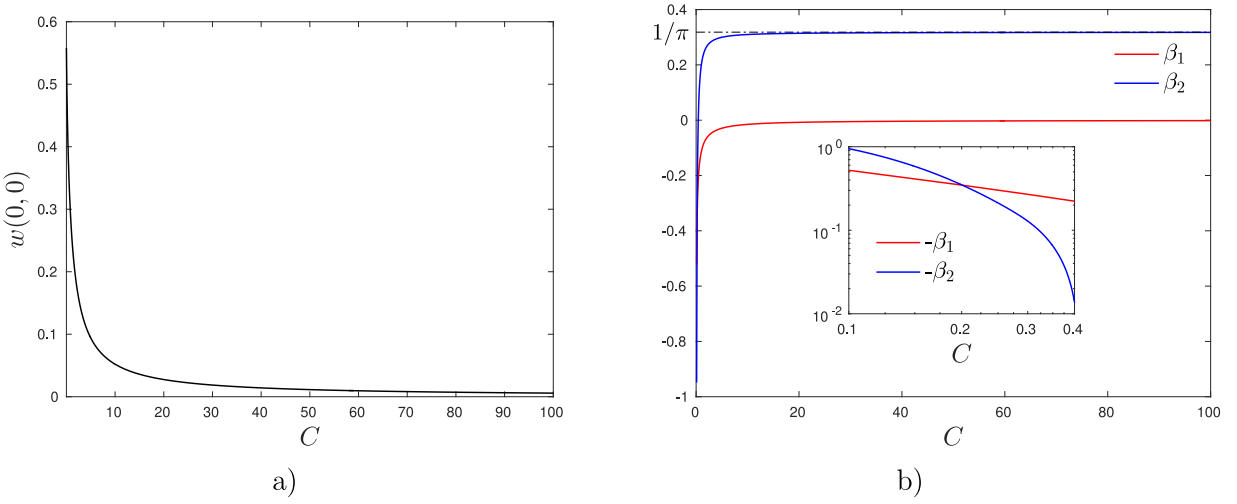

Fig. 3. Logarithmic singularity (Section 4.1). Dependence of different quantities on parameters C a) displacement at $r=0$, $\theta=0$ according to (62), b) coefficients of asymptotic expansion from (63).

Only in this case, the stress near the crack tip is bounded, while when $0<C<\infty$, the stress demonstrate log singularity near this point. Coefficient in the front of this term is shown on the Fig. 3.

Let us now turn to presentation of the results for the alternative case described in Section 4.2. The corresponding stresses and displacements are shown in Fig. 4. Now, the singular point appears at $r=1$. Interestingly, both solutions from the in Sections 4.1 and 4.2 coincide in the limiting case $C=\infty$ regardless of the load (even if $F^{+}(0)\neq 0$) as it clearly follows from (54).

Finally, we illustrate both solutions by comparing the force balance conditions (70) and (57). In more details, we present in Fig. 5 total stress $\Sigma^{\pm}(0)$ and their sum (solid bold line). One can see that the balance condition (70) satisfies for the first solution ($G(1)=1$), but not for the second one due to aforementioned appearance of the point forces at zero point (at the corner of the domain).

6. Solution for asymmetric problem

6.1. Reduction to the Wiener–Hopf problem

General comment - solution cannot be found in unique way (at least adding a constant to the solution w change nothing in formulation (apart from the behaviour at infinity). For this reason, we again search for solution vanishing at infinity.

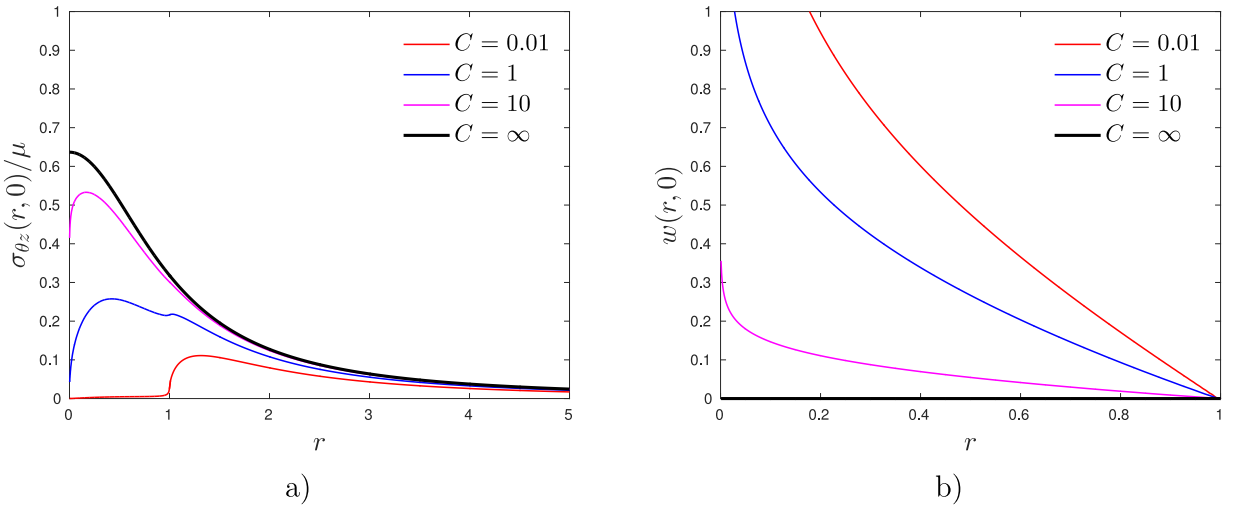

Fig. 4. Bounded solution (Section 4.2). Distribution of stress and displacements according to the alternative solution in (65) and different values of C: a) normalized stress, b) displacements.

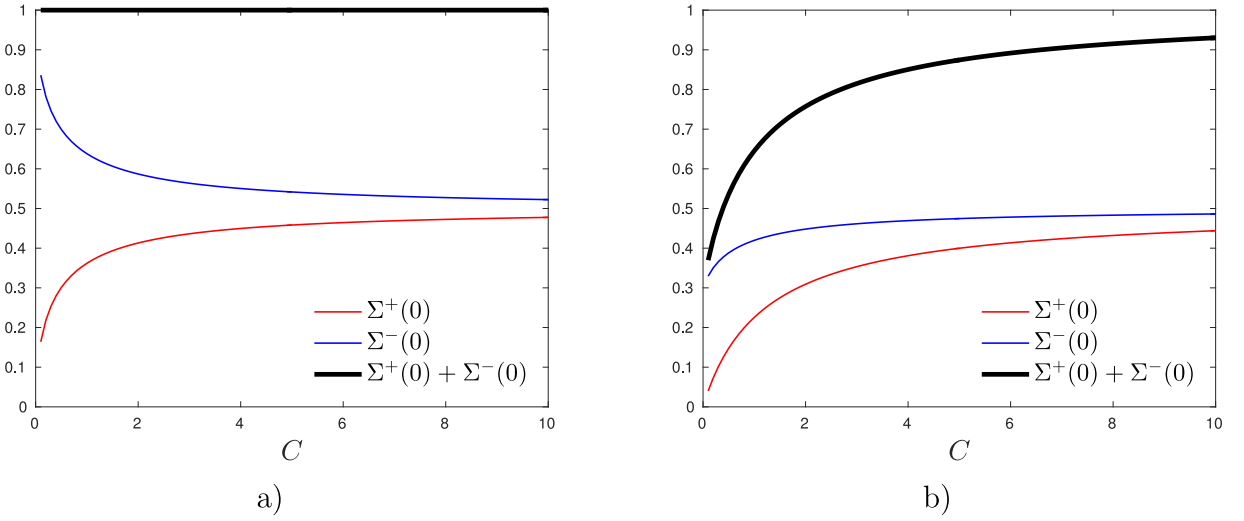

Fig. 5. Bounded solution (Section 4.2). Total force comparison for different solutions and different values of C: a) principal solution (65), b) alternative solution (65).

Let's write the boundary conditions in the form defined along the entire ray $0 < r < \infty$:

$$\mu \frac{\partial w}{\partial \theta} = rg(r), \quad \theta = \frac{\pi}{2},$$
$$\mu \frac{\partial w}{\partial \theta} + Cr \frac{\partial}{\partial r}\left(r \frac{\partial w}{\partial r}\right) = rh(r) + \phi(r), \quad \mu \frac{\partial w}{\partial \theta} = \psi(r), \quad \theta = 0. \tag{79}$$

where the given function $h(r)$ satisfies the condition $h(r) = 0$ for $r > 1$ and newly introduced unknown functions assume

$$\phi(r) = 0, \quad 0 < r < 1, \qquad \psi(r) = 0, \quad r > 1. \tag{80}$$

Applying again the Mellin transform we will get (17) and the last condition changes to:

$$\mu W'_\theta + Cs^2 W = H^+(s+1) + \Phi^-(s), \quad \mu W'_\theta = \Psi^+(s), \quad \theta = 0. \tag{81}$$

Here, we preserve the same notations for given functions.

Substituting (30) into the boundary conditions along the ray $\theta = 0$ now we have:

$$\begin{pmatrix} A(s) \\ B(s) \end{pmatrix} = \begin{pmatrix} \sin\frac{\pi s}{2} & \cos\frac{\pi s}{2} \\ \cos\frac{\pi s}{2} & -\sin\frac{\pi s}{2} \end{pmatrix} \begin{pmatrix} \frac{1}{\mu s}\Psi^+(s) \\ \frac{1}{Cs^2}\big(\Phi^-(s) + H^+(s+1) - \Psi^+(s)\big). \end{pmatrix} \tag{82}$$

This brings us to the Wiener–Hopf equation:

$$\frac{G(s+1)}{\cos\frac{\pi s}{2}} + \frac{\mu}{C}M(s)H^+(s+1) = L(s)\Psi^+(s) - \frac{\mu}{C}M(s)\Phi^-(s), \tag{83}$$

valid in the strip $-\alpha_0 < \Re s < \alpha_\infty$. Here the kernel function $L(s)$ is the same as in (35) and:

$$M(s) = \frac{1}{s}\tan\frac{\pi s}{2}. \tag{84}$$

Note that our assumptions (21)–(23) and (24)–(27) are consistent with (34) and the following conclusions can be made from its analysis at point $s = 0$:

$$G(1) = \Phi^-(0) + H^+(1), \quad \Psi^+(0) = G(1), \quad w_0 = \frac{1}{C}\frac{d}{ds}\big(\Phi^-(s) + H^+(s+1) - \Psi^+(s)\big)\Big|_{s=0}. \tag{85}$$

The first and the second equations in the latter are nothing but equivalent forms of the balance condition (29). Finally, in the preliminary analysis of the Wiener–Hopf equation it follows that $\alpha_0 = \alpha_\infty = 1$.

6.2. Solution to the Wiener–Hopf equation and it analysis

Note that the function $M(s)$ can be easy factorized analytically in closed form $M(s) = M^+(s)M^-(s)$ where $M^+(s) = M^-(-s)$, $M^+(s)$ is analytical in the half-plane $\Re s > -1$ and

$$M^\pm(0) = \sqrt{\frac{\pi}{2}}, \quad M^\pm(s) \sim (\pm s)^{-1/2}, \quad \Re s \to \pm\infty.$$

As a result the Wiener–Hopf Eq. (34) can be rewritten in the form:

$$\frac{L^+(s)}{M^+(s)}\Psi^+(s) - \frac{\mu}{C}\frac{M^-(s)}{L^-(s)}\Phi^-(s) = K(s), \tag{86}$$

where

$$K(s) = \frac{1}{M^+(s)L^-(s)}\left(\frac{G(s+1)}{\cos\frac{\pi s}{2}} + \frac{\mu}{C}M(s)H^+(s+1)\right). \tag{87}$$

Assuming function $H^+(s+1)$ behaves not bad we have:

$$K^\pm(s) = \mp\frac{1}{2\pi i}\int_{-i\infty\mp\gamma}^{i\infty\mp\gamma}\frac{K(\xi)}{\xi - s}d\xi, \tag{88}$$

where $0 \le \gamma < 1$ is an arbitrary constant. Solution to the Eq. (86) can be found in the form:

$$\frac{L^+(s)}{M^+(s)}\Psi^+(s) - K^+(s) = \frac{\mu}{C}\frac{M^-(s)}{L^-(s)}\Phi^-(s) + K^-(s) \equiv \mathcal{P}_n(s), \tag{89}$$

in the strip $0 < \Re s < 1$, where $\mathcal{P}_n(s)$ is a polynomial.

As the result, the final solution of the Wiener–Hopf equation is:

$$\Psi^+(s) = \frac{M^+(s)}{L^+(s)}\big(\mathcal{P}_n(s) + K^+(s)\big), \quad \Phi^-(s) = \frac{CL^-(s)}{\mu M^-(s)}\big(\mathcal{P}_n(s) - K^-(s)\big). \tag{90}$$

We can compute the sought for Mellin images of displacements and stress along the line $\theta = 0$ described in the domain $0 < \Re s < 1$ (to preserve the proper behaviour at infinity):

$$W(s,0) = \frac{1}{\mu s\tan\frac{\pi s}{2}}\left(\Psi^+(s) - \frac{G(s+1)}{\cos\frac{\pi s}{2}}\right), \quad \mu\frac{\partial}{\partial\theta}W(s,0) = \Psi^+(s). \tag{91}$$

This, in turn allows us to conclude that the polynomial should be a constant only $\mathcal{P}_n(s) = P_0$. To satisfy balance condition (and it eliminates the $\log r$ term at zero point in displacement), we need to satisfy the condition $(85)_2$ or

$$\frac{M^+(0)}{L^+(0)}\big(P_0 + K^+(0)\big) = G(1). \tag{92}$$

As a result,

$$\Psi^+(s) = \frac{M^+(s)}{L^+(s)}\left(\frac{L^+(0)}{M^+(0)}G(1) - K^+(0) + K^+(s)\right). \tag{93}$$

Analyzing the behaviour at infinity we can conclude that

$$w(r,0) = O(|1-r|^{1/2}), \quad r \to 1, \quad \sigma_{z\theta}(r,0) = O((r-1)^{-1/2}), \quad r \to 1-,$$

or more accurately,

$$\sigma_{\theta z}(r.0) \sim \frac{k_3}{\sqrt{1-r}}, \quad r \to 1-, \quad k_3 = \frac{P_0}{\sqrt{\pi}} = \frac{1}{\sqrt{\pi}}\left(\frac{L^+(0)}{M^+(0)}G(1) - K^+(0)\right).$$

If by a chance $P_0 = 0$ or:

$$\frac{M^+(0)}{L^+(0)}K^+(0) = \sqrt{\frac{C\pi}{2C+\mu\pi}}K^+(0) = G(1), \tag{94}$$

then there is no singularity at the crack tip. Note that the (94) is always possible to satisfy. For example, taking $h(r) = 0$ and $g(r) = D_1\delta(r-a_1) + D_2\delta(r-a_2)$. However, it is clear that at least on of the constants defining function $g(r)$ will depend on C.

6.3. Discussion on the solution expected behaviour when ($C \to \infty$ and $C \to 0$)

When $C \to \infty$ then $K(s), K^{\pm}(s) = O(1)$, the same property can be checked for the function $\Psi^+(s)$. One can check that this solution has a direct limit (corresponding to the problem with the condition $w(r,0) = 0$ for $0 < r < 1$ and the semi-infinite crack on $1 < r < \infty$ free of load.

In the opposite limiting case we have

$$K(s) = O(C^{-1/2}), \quad K^{\pm}(s) = O(C^{-1/4}), \quad C \to 0, \quad \text{if} \quad h(r) \equiv 0,$$

or

$$K(s) = O(C^{-3/2}), \quad K^{\pm}(s) = O(C^{-3/4}), \quad C \to 0, \quad \text{if} \quad h(r) \neq 0,$$

thus those two cases should be considered separately.

In the first ($h(r) \equiv 0$), we have $\Psi^+(s) = O(s^{1/4})$, $P_0 = O(s^{-1/2})$ as $C \to 0$. As a result, we can expect that while the stress vanishes along the interval $0 < r < 1$, it blows up near the point $r = 1$ when the stress intensity factor dramatically increases ($k_3 = O(s^{-1/2})$).

In the second case ($h(r) \equiv 0$), we conclude that $\Psi^+(s) = O(s^{-1/4})$, $P_0 = O(s^{-1/2})$ as $C \to 0$. Thus, both, the stress along the interval $0 < r < 1$ and the stress intensity factor frows dramatically.

Note that these conclusions were made after assumption that the given load is fixed while the constant C changes. If the load is following the value of C to satisfy (94), statements related to the value of the stress intensity factors will change. In addition we finally note, that all those propositions on the possible behaviour of the problem in limiting cases are not exact and the estimates given are not uniform.

7. Concluding remarks

In the framework of the linear Gurtin–Murdoch model of surface elasticity we presented full solution of mode III crack problem. In order to analyze effects of surface stresses near the crack tip we assume linear dependence of the surface shear modulus on the coordinate along the surface $\mu_s = f(x)$ such that it has maximum value at the crack tip and vanishes at the point where the crack ends at the boundary. Note that the case $f(x) = C \equiv \text{const}$ with $g_{\pm}(y) = 0$ and $h_+(x) = h_-(x)$ corresponds to the aforementioned configuration considered by Kim et al. (2010a, 2010b, 2011b). Using the integral transformations technique the analysis yields nonsingular stress and displacements distributions.

We have already mentioned in the introduction certain controversies concerning the near-tip asymptotics in case of surface stresses at crack surfaces, see Kim et al. (2011c), Kim, Schiavone, and Ru (2011a), Wang et al. (2011), Walton (2012) and Xu and Dong (2016). Namely, even for mode III some papers stated that traction is bounded, see Kim et al. (2010a, 2010b, 2011b), while other works found log singularity (Kim et al., 2013; Walton, 2012; Wang & Schiavone, 2016b) or the classic square root singularity (Li, 2019). In the present work focused on a specific geometry, we show that there is actually no a controversy in this issue: the singularity exists if some additional loading and geometry conditions are not fulfilled.

Specifically, we have demonstrated that in the problem under consideration, depending on the certain conditions on the applied load, the solution may be finite near the crack tip, or has the logarithmic or even the square root singularity. Physically, this can be explained by the fact that the Gurtin–Murdoch model is mathematically equivalent to a stiff elastic surface coating (Mishuris, 2003; Mishuris et al., 2006b; 2010). This, in turn, clearly constrains one type of loading but may invoke an additional effects for another loading resulting in the surface bending. The Gurtin–Murdoch model has been further extended to more general surface-related constitutive equations by Steigmann and Ogden (1997, 1999), where the resistance to surface bending is considered, and some others, see, e.g., Povstenko (1991), Lurie, Volkov-Bogorodsky, Zubov, and Tuchkova (2009), Javili, Mc Bride, and Steinmann (2013b), Javili, dell'Isola, and Steinmann (2013a), Belov, Lurie, and Golovina (2019) and Eremeyev (2019), and references therein. It would be interesting to analyze near tip asymptotics for a crack with more sophisticated models of surface elasticity as Steigmann–Ogden one (see relevant works by Zemlyanova (2016, 2017) and Han, Mogilevskaya, and Schillinger (2018)).

Declaration of Competing Interest

The authors declare that there is no conflict of interest.

Acknowledgements

V.A.E. acknowledges the support by grant 14.Z50.31.0036 awarded to R. E. Alekseev Nizhny Novgorod Technical University by Department of Education and Science of the Russian Federation. GM acknowledges financial support from the ERC Advanced Grant "Instabilities and nonlocal multiscale modelling of materials", ERC-2013-ADG-340561-INSTABILITIES. He is also thankful to the Royal Society for the Wolfson Research Merit Award and the Isaac Newton Institute for Mathematical Sciences (INI) for Simon's Fellowship. NG and GM would like to thank INI, Cambridge, for support (through the EPSRC grant no EP/R014604/1) and hospitality during the programme "Bringing pure and applied analysis together via the Wiener-Hopf technique, its generalisations and applications" where work on this paper was completed. NG acknowledges the support of the French Agence Nationale de la Recherche (ANR) under reference ANR-17-CE08-0047-02.

Appendix A. Complete solution for the limit case C=0

Herewith, we present the solution of a conventional problem with an edge crack. This scenario corresponds to the symmetric case $[w]=0,\ r>1,\ \theta=0$, referring to terminology of the main body of the work. For simplicity, we also consider case $h(r)=0$. We define functions:

$$\Phi^-(s)=\int_1^\infty \mu\frac{\partial w}{\partial\theta}(r,0)r^{s-1}\,dr,\qquad \Psi^+(s)=\int_0^1 w(r,0)r^{s-1}\,dr.$$

Symbol $+$ refers to the complex valued functions analytic in domain $\Re s>\beta$ with $\beta>0$ whereas symbol $-$ stands for functions analytic in $\Re s<0$. Application of the remaining boundary conditions (15) in case $C=0$:

$$\begin{aligned}&A(s)\mu s\sin\left(\frac{\pi s}{2}\right)+\frac{G(s+1)}{s}\mu s\cos\left(\frac{\pi s}{2}\right)=\Phi^-(s),\\&A(s)\cos\left(\frac{\pi s}{2}\right)-\frac{G(s+1)}{s}\sin\left(\frac{\pi s}{2}\right)=\Psi^+(s).\end{aligned}\tag{A.1}$$

Eliminating $A(s)$ from the last system reduces it to the Wiener–Hopf problem:

$$\frac{\mu}{\cos\left(\frac{\pi s}{2}\right)}G(s)=\Phi^-(s)-s^2L(s)\Psi^+(s).\tag{A.2}$$

The kernel function of the problem is defined as:

$$L(s)=\mu\frac{\tan\left(\frac{\pi s}{2}\right)}{s}.$$

We expect the following behaviour of functions:

$$\begin{aligned}\Psi^+(s)&=O\big(s^{-1}\big),\quad s\to 0,\\ \Psi^+(s)=O\big(|s|^{-3/2}\big),\quad \Phi^-(s)&=O\big(|s|^{-1/2}\big),\quad s\to\infty.\end{aligned}\tag{A.3}$$

Kernel functions behaves as follows:

$$L(s)=\frac{\mu\pi}{2}+O\big(s^2\big),\quad s\to 0,\qquad L(\pm i\xi)\sim -i\frac{\mu}{\xi},\quad \xi\to\infty.\tag{A.4}$$

Let us use the facts that:

$$\begin{aligned}&\Gamma\Big(\frac{2-z}{2}\Big)\Gamma\Big(\frac{z}{2}\Big)=\frac{\pi}{\sin\frac{\pi z}{2}},\quad \Gamma\Big(\frac{1-z}{2}\Big)\Gamma\Big(\frac{1+z}{2}\Big)=\frac{\pi}{\cos\frac{\pi z}{2}},\\&z\Gamma(z)=\Gamma(z+1),\end{aligned}$$

where $\Gamma(z)$ is the Gamma function, analytic in the half-plane $\Re(z)>0$. Hence:

$$\tan\frac{\pi s}{2}=\frac{s}{2}\frac{\Gamma\left(\frac{1-z}{2}\right)\Gamma\left(\frac{1+z}{2}\right)}{\Gamma\left(\frac{2-z}{2}\right)\Gamma\left(\frac{2+z}{2}\right)}$$

Function $L(s)$ can be factorized as follows:

$$L(s)=L^+(s)L^-(s),\quad L^\pm(s)=\sqrt{\frac{\mu}{2}}\Gamma\Big(\frac{1\pm s}{2}\Big)\Gamma^{-1}\Big(\frac{2\pm s}{2}\Big)\tag{A.5}$$

Recall Stirling's formula:

$$\Gamma(z+1) \sim \sqrt{2\pi z}\left(\frac{z}{e}\right)^z, \quad z \to \infty$$

Functions $L^{\pm}(s)$ has the following asymptotic behaviour:

$$L^{\pm}(s) = \sqrt{\frac{\mu\pi}{2}} + o(1), \quad s \to 0, \qquad L^{\pm}(s) = \sqrt{\frac{\mu}{\pm s}}\left(1 \mp \frac{1}{4s} + O\left(\frac{1}{s^2}\right)\right), \quad s \to \pm\infty. \tag{A.6}$$

We get:

$$\frac{\Phi^-(s)}{L^-(s)} - s^2\Psi^+(s)L^+(s) = F(s), \qquad F(s) = \frac{\mu}{\cos\frac{\pi s}{2}}\frac{G(s+1)}{L^-(s)}. \tag{A.7}$$

Function $F(s)$ is presented as follows:

$$F(s) = F^+(s) + F^-(s), \quad F^{\pm}(s) = \mp\frac{1}{2\pi i}\int_{-i\infty}^{i\infty}\frac{F(p)}{p-s}\,dp, \tag{A.8}$$

where $F^{\pm}(s) = O(|s|^{-1})$, $s \to \infty$. Then, we conclude:

$$\frac{\Phi^-(s)}{L^-(s)} - F^-(s) = s^2\Psi^+(s)L^+(s) + F^+(s) \equiv D_0 + D_1 s. \tag{A.9}$$

Coefficients $D_{0,1}$ and chosen in such a way to get the desired behaviour of displacements and stresses. We finally arrive to the following solution:

$$\Phi^- = \big(F^-(s) + F^+(0)\big)L^-(s), \qquad \Psi^+(s) = -\frac{F^+(s) - F^+(0)}{s^2L^+(s)}. \tag{A.10}$$

Thus, we may obtain:

$$A(s) = \frac{G(s+1)}{s}\tan\frac{\pi s}{2} - \frac{1}{\cos\frac{\pi s}{2}}\Psi^+(s), \tag{A.11}$$

and, similarly to the previous more general case:

$$W(s,\theta) = \Psi^+(s)\cos\theta s + \left(\Psi^+(s)\tan\frac{\pi s}{2} + \frac{B(s)}{\cos\frac{\pi s}{2}}\right)\sin\theta s \tag{A.12}$$

When $\theta = 0$ we directly obtain:

$$W(s,0) = \Psi^+(s), \quad \mu\frac{\partial W}{\partial\theta}(s,0) = \Phi^-(s). \tag{A.13}$$

Supplementary material

Supplementary material associated with this article can be found, in the online version, at doi:10.1016/j.ijengsci.2019.103183.

References

Antipov, Y. A., & Schiavone, P. (2011). Integro-differential equation for a finite crack in a strip with surface effects. *Quarterly Journal of Mechanics and Applied Mathematics, 64*(1), 87–106.

Barenblatt, G. I. (1959). The formation of equilibrium cracks during brittle fracture. General ideas and hydrotheses: Axially-symmetric cracks. *Journal of Applied Mathematicsand Mechanics, 23*, 622–636.

Belov, P. A., Lurie, S. A., & Golovina, N. Y. (2019). Classifying the existing continuum theories of ideal-surface adhesion. In *Adhesives and adhesive joints in industry* (pp. 1–12). IntechOpen.

Benveniste, Y., & Miloh, T. (2001). Imperfect soft and stiff interfaces in two-dimensional elasticity. *Mechanics of Materials, 33*(6), 309–323.

Benveniste, Y., & Miloh, T. (2007). Soft neutral elastic inhomogeneities with membrane-type interface conditions. *Journal of Elasticity, 88*(2), 87–111.

Duan, H. L., Wang, J., & Karihaloo, B. L. (2008). Theory of elasticity at the nanoscale. In *Advances in applied mechanics: 42* (pp. 1–68). Elsevier.

Eremeyev, V. A. (2016). On effective properties of materials at the nano-and microscales considering surface effects. *Acta Mechanica, 227*(1), 29–42.

Eremeyev, V. A. (2019). Strongly anisotropic surface elasticity and antiplane surface waves. *Philosophical Transactions of the Royal Society A*, 1–14.

Eremeyev, V. A., & Lebedev, L. P. (2013). Existence of weak solutions in elasticity. *Mathematics and Mechanics of Solids, 18*(2), 204–217.

Eremeyev, V. A., & Lebedev, L. P. (2016). Mathematical study of boundary-value problems within the framework of Steigmann–Ogden model of surface elasticity. *Continuum Mechanics and Thermodynamics, 28*(1–2), 407–422.

Gurtin, M. E., & Murdoch, A. I. (1975). A continuum theory of elastic material surfaces. *Archive for Rational Mechanics and Analysis, 57*(4), 291–323.

Gurtin, M. E., & Murdoch, A. I. (1978). Surface stress in solids. *International Journal of Solidsand Structures, 14*(6), 431–440.

Han, Z., Mogilevskaya, S. G., & Schillinger, D. (2018). Local fields and overall transverse properties of unidirectional composite materials with multiple nanofibers and Steigmann–Ogden interfaces. *International Journal of Solids and Structures, 147*, 166–182.

Javili, A., dell'Isola, F., & Steinmann, P. (2013). Geometrically nonlinear higher-gradient elasticity with energetic boundaries. *Journal of the Mechanicsand Physicsof Solids, 61*(12), 2381–2401.

Javili, A., Mc Bride, A., & Steinmann, P. (2013). Thermomechanics of solids with lower-dimensional energetics: on the importance of surface, interface, and curve structures at the nanoscale. A unifying review. *Applied Mechanics Reviews, 65*(1), 010802.

Kim, C., Schiavone, P., & Ru, C. Q. (2011). Analysis of plane-strain crack problems (mode-I & mode-II) in the presence of surface elasticity. *Journal of Elasticity, 104*(1–2), 397–420.
Kim, C. I., Ru, C. Q., & Schiavone, P. (2013). A clarification of the role of crack-tip conditions in linear elasticity with surface effects. *Mathematics and Mechanics of Solids, 18*(1), 59–66.
Kim, C. I., Schiavone, P., & Ru, C. Q. (2010). Analysis of a mode-III crack in the presence of surface elasticity and a prescribed non-uniform surface traction. *Zeitschrift für angewandte Mathematik und Physik, 61*(3), 555–564.
Kim, C. I., Schiavone, P., & Ru, C. Q. (2010). The effects of surface elasticity on an elastic solid with mode-III crack: complete solution. *Transactions of ASME Journal of Applied Mechanics, 77*(2), 021011.
Kim, C. I., Schiavone, P., & Ru, C. Q. (2011). The effect of surface elasticity on a mode-III interface crack. *Archives of Mechanics, 63*(3), 267–286.
Kim, C. I., Schiavone, P., & Ru, C. Q. (2011). Effect of surface elasticity on an interface crack in plane deformations. *Proceedings of the Royal Society A, 467*(2136), 3530–3549.
Li, X. F. (2019). Effect of surface elasticity on stress intensity factors near mode-III crack tips. *Journal of Mechanics of Materials and Structures, 14*(1), 43–60.
Lurie, S., Volkov-Bogorodsky, D., Zubov, V., & Tuchkova, N. (2009). Advanced theoretical and numerical multiscale modeling of cohesion/adhesion interactions in continuum mechanics and its applications for filled nanocomposites. *Computational Materials Science, 45*(3), 709–714.
Mishuris, G., Öchsner, A., & Kuhn, G. (2006). FEM-analysis of nonclassical transmission conditions between elastic structures. Part 2: Stiff imperfect interface. *CMC: Computers, Materials, & Continua, 4*(3), 137–152.
Mishuris, G. S. (2003). Mode III interface crack lying at thin nonhomogeneous anisotropic interface. Asymptotics near the crack tip. In *IUTAM symposium on asymptotics, singularities and homogenisation in problems of mechanics* (pp. 251–260). Springer.
Mishuris, G. S., Movchan, N. V., & Movchan, A. B. (2006). Steady-state motion of a mode-III crack on imperfect interfaces. *The Quarterly Journal of Mechanics & Applied Mathematics, 59*(4), 487–516.
Mishuris, G. S., Movchan, N. V., & Movchan, A. B. (2010). Dynamic mode-III interface crack in a bi-material strip. *International Journal of Fracture, 166*(1–2), 121–133.
Piccolroaz, A., & Mishuris, G. (2013). Integral identities for a semi-infinite interfacial crack in 2D and 3D elasticity. *Journal of Elasticity, 110*(2), 117–140.
Piccolroaz, A., Mishuris, G., & Movchan, A. B. (2009). Symmetric and skew-symmetric weight functions in 2D perturbation models for semi-infinite interfacial cracks. *Journal of the Mechanics and Physics of Solids, 57*(9), 1657–1682.
Povstenko, Y. Z. (1991). Generalizations of laplace and young equations involving couples. *Journal of Colloid and Interface Science, 144*(2), 497–506.
Ru, C. Q. (2010). Simple geometrical explanation of Gurtin–Murdoch model of surface elasticity with clarification of its related versions. science china physics. *Mechanics and Astronomy, 53*(3), 536–544.
Schiavone, P., & Ru, C. Q. (2009). Solvability of boundary value problems in a theory of plane-strain elasticity with boundary reinforcement. *International Journal of Engineering Science, 47*(11), 1331–1338.
Sigaeva, T., & Schiavone, P. (2014). Solvability of a theory of anti-plane shear with partially coated boundaries. *Archives of Mechanics, 66*(2), 113–125.
Steigmann, D. J., & Ogden, R. W. (1997). Plane deformations of elastic solids with intrinsic boundary elasticity. *Proceedings of the Royal Society A, 453*(1959), 853–877.
Steigmann, D. J., & Ogden, R. W. (1999). Elastic surface-substrate interactions. *Proceedings of the Royal Society A, 455*(1982), 437–474.
Walton, J. R. (2012). A note on fracture models incorporating surface elasticity. *Journal of Elasticity, 109*(1), 95–102.
Wang, C., & Wang, X. (2017). A mode III rate-dependent bridged crack with surface elasticity. *Mechanics of Materials, 108*, 107–119.
Wang, J., Huang, Z., Duan, H., Yu, S., Feng, X., Zhang, G., Wang, W., & Wang, T. (2011). Surface stress effect in mechanics of nanostructured materials. *Acta Mech. Solida Sinica, 24*, 52–82.
Wang, X. (2015). A mode III arc-shaped crack with surface elasticity. zeitschrift für angewandte. *Mathematik und Physik, 66*(4), 1987–2000.
Wang, X., & Schiavone, P. (2015). Two circular inclusions with arbitrarily varied surface effects. *Acta Mechanica, 226*(5), 1471–1486.
Wang, X., & Schiavone, P. (2016). Bridged cracks of mode III with surface elasticity. *Mechanics of Materials, 95*, 125–135.
Wang, X., & Schiavone, P. (2016). A mode-III crack with variable surface effects. *Journal of Theoretical and Applied Mechanics, 54*(4), 1319–1327.
Xu, J. Y., & Dong, C. Y. (2016). Surface and interface stress effects on the interaction of nano-inclusions and nano-cracks in an infinite domain under anti-plane shear. *International Journal of Mechanical Sciences, 111*, 12–23.
Zemlyanova, A. Y. (2016). Curvilinear mode-I/mode-II interface fracture with a curvature-dependent surface tension on the boundary. *IMA Journal of Applied Mathematics, 81*(6), 1112–1136.
Zemlyanova, A. Y. (2017). A straight mixed mode fracture with the Steigmann–Ogden boundary condition. *The Quarterly Journal of Mechanics and Applied Mathematics, 70*(1), 65–86.